Effect of Mutation of the Sac7d Intercalating Residues on the Temperature Dependence of DNA Distortion and Binding Thermodynamics†

William B. Peters, Stephen P. Edmondson,* and John W. Shriver*

Laboratory for Structural Biology, Departments of Chemistry and Biological Sciences, Graduate Program in Biotechnology and Bioengineering, University of Alabama, Huntsville, Alabama 35899

Received December 13, 2004; Revised Manuscript Received January 24, 2005

ABSTRACT: Sac7d is a small chromatin protein from the hyperthermophile *Sulfolobus acidocaldarius* which kinks duplex DNA by ∼66° at a single base pair step with intercalation of V26 and M29 side chains. Site-directed mutagenesis coupled with calorimetric and spectroscopic data has been used to characterize the influence of the intercalating side chains on the structure and thermodynamics of the DNA complex from 5 to 85 °C. Two single-alanine substitutions (V26A and M29A) and five double-glycine, -alanine, -leucine, -phenylalanine, and -tryptophan substitutions of the surface residues have been created. NMR and fluorescence titrations indicated that the substitutions had little effect on the structure of the protein or DNA binding site size. Each of the mutant proteins demonstrated a temperature-dependent binding enthalpy which was correlated with a similar temperature dependence in the structure of the complex reflected by changes in fluorescence and circular dichroism. A positive heat capacity change (ΔC_p) for DNA binding was observed for only those mutants which also demonstrated a thermotropic structural transition in the complex, and the temperature range for the positive ΔC_p coincided with that observed for the structural transition. The thermodynamic data are interpreted using a model in which binding is linked to an endothermic distortion of the DNA in the complex. The results support the proposal that the unfavorable enthalpy of binding of Sac7d at 25 °C is due in part to the distortion of DNA.

The bending of DNA is an important function of many DNA binding proteins involved in both chromatin packaging and gene regulation (*1*−*6*). Significant bending with roll angles greater than 20° has been documented in both sequence specific and non-sequence specific DNA-binding proteins, including major groove binding proteins such as CAP and EcoRI, as well as minor groove binding proteins such as TBP, IHF, HMGB, and Sac7d (*7*−*10*). For many of these, DNA bending is associated with intercalation of hydrophobic residues into DNA at specific kink sites (*4*, *11*, *12*). In such structures, intercalating side chains appear to function as wedges which pry open the DNA structure. In others, there is little or no intercalation, and bending must be dictated by other factors, including DNA sequence and its proclivity to bend (*13*). Protein-induced redistribution of charge on the DNA as a result of protein binding can also play a role (*14*).

There must be an energetic penalty associated with bending DNA since prebending can promote enhanced binding of some proteins (*15*, *16*). Arguments have been presented which indicate that the penalty of bending DNA is reflected in the enthalpy of binding. Jen-Jacobson et al. (*17*) noted that the heats of binding of a select group of DNA binding proteins at 25 °C appeared to be correlated with the degree of bending. Proteins which significantly bent DNA showed a more positive enthalpy of binding than those that did not. The unfavorable enthalpy was attributed to "strain" forced into the DNA due to bending. A comparison of the thermodynamics of binding by more than 20 proteins over a range of temperatures indicates that bending leads to an ∼10−15 kcal/mol increase in enthalpy (*18*). However, because of the widely differing values for the ΔC_p of binding, the ordering of the proteins is very much dependent on the choice of temperature.

A quantitative correlation between binding enthalpy and distortion requires a system in which it is possible to vary the DNA distortion and measure the associated changes in the energetics of binding. We have presented evidence which indicates that the small DNA binding protein Sac7d may permit such measurements with DNA bend angles approaching 70° and no associated change in protein structure (*12*, *18*, *19*). Non-sequence specific DNA binding by this hyperthermophile protein allows assessment of binding over an unusually wide temperature range because of the high thermal stability of both the protein and extended synthetic DNA duplexes. This permits the separation of the thermodynamics of protein−DNA binding from protein and DNA folding, and eliminates the need to correct calorimetric (ITC) binding data with results from heat capacity (DSC) measurements to adjust for unfolding of protein and DNA over the temperature range used to characterize binding (*10*, *20*).

The enthalpy of Sac7d−DNA binding is unfavorable and is consistent with that observed for many other DNA-binding proteins which distort DNA (*17*, *18*). However, substitution

† This work was supported by Grant GM49686 from the National Institutes of Health to J.W.S. and S.P.E.

* To whom correspondence should be addressed: Department of Chemistry, Materials Science Building, John Wright Drive, University of Alabama, Huntsville, AL 35899. Phone: (256) 824-2477. Fax: (256) 824-6349. E-mail: shriverj@uah.edu or edmonds@uah.edu.

10.1021/bi047382w CCC: $30.25
Published on Web 03/02/2005

of both the intercalating residues in Sac7d with alanine led to only a small decrease in the heat of binding, even though spectroscopic and structural data indicated that this protein induced significantly less distortion (*18*). The spectroscopic changes induced by the protein were temperature-dependent and consistent with an increased level of distortion at higher temperatures. In addition, the heat of DNA binding increased with temperature and could be explained by a temperature-dependent structural change in the protein−DNA complex, and not in the free protein or DNA. The data were consistent with an endothermic distortion of the protein-bound DNA with a T_m[1] around 15 °C. In this interpretation, the hydrophobic V26 and M29 intercalating side chains in the native protein stabilize the distorted DNA and therefore shift the T_m for the bending to a lower temperature. The double-alanine mutation would appear to position the T_m near 15 °C and conveniently allow a study of the temperature dependence of the transition. To test this interpretation, we have extended this work to other mutations of the intercalating residues. The goal was to determine if other substitutions of the intercalating residues could position the apparent T_m of the transition in the complex above or below that observed for the double-alanine mutant. Most importantly, the temperature dependence of the heat of binding should correlate with a similar temperature dependence of the structure reflected by changes in the CD and fluorescence spectra of the complex. We show here that this is the case, and conclude that the unfavorable enthalpy of Sac7d−DNA binding can be attributed in part to the distortion of DNA.

EXPERIMENTAL PROCEDURES

Materials. Sac7d and mutant proteins were expressed in *Escherichia coli* strains BL21(DE3)pLysS and RosettaBlue-(DE3)pLysS. The proteins were purified as previously described for Sac7d (*21*). Proteins used to collect $^1H-^{15}N$ HSQC NMR spectra were labeled with ^{15}N by expression in minimal media supplemented with $^{15}NH_4Cl$ (*22*). Site-directed mutations were introduced using the CLONETECH (Palo Alto, CA) Transformer Kit, and mutations were verified by both DNA sequencing and mass spectrometry. Protein concentrations were determined using an extinction coefficient at 280 nm of 1.1 mL mg^{-1} cm^{-1} for all proteins (*23*). Differences in 280 nm extinction due to site specific mutations characterized in this work were assumed to be negligible and within the error of that determined for Sac7d.

Synthetic duplex poly(dGdC) was purchased from Pharmacia (Piscataway, NJ) with an average length of 1000 bp as determined by agarose gel electrophoresis. The concentration of poly(dGdC) (in bases) was determined spectrophotometrically using an extinction coefficient at 254 nm of 8400 M^{-1} cm^{-1}.

Fluorescence. Fluorescence measurements were performed on SLM 8000C and Fluoromax-3 fluorimeters with temperature control to within ±0.2 °C. DNA titrations were performed as described previously (*24*) by monitoring the intrinsic tryptophan fluorescence with excitation at 295 nm (4 nm slit) and emission at 345 nm (8 nm slit). Aliquots (5 μL) of a concentrated nucleotide solution (1 mM in 0.01 M KH_2PO_4 and 0.025 M KCl at pH 7) were titrated into protein (0.5−5 μM, in identical buffer) in a 4 mL quartz fluorescence cell with stirring.

Binding parameters were obtained by fitting the dependence of the observed tryptophan fluorescence quenching on the total DNA concentration using in-house nonlinear regression programs based on the Marquardt algorithm (*25*). The binding site size (n), binding affinity (K), and maximal quenching (Q_{max}) were obtained by minimizing the error function

$$\chi^2 = \sum_i [Q(i)_{obs} - Q(i)_{calc}]^2 \quad (1)$$

where the sum is over all i data points in a titration. The observed quenching, Q_{obs}, is defined as $(F - F_{obs})/F$, where F is the fluorescence intensity of the protein in the absence of DNA and F_{obs} is the experimentally observed fluorescence with a total DNA concentration of L_t. Q_{calc} is the calculated fluorescence quenching given by $Q_{max}L_b/L_t$. The concentration of bound protein L_b resulting from given total DNA (D_t) and protein (L_t) concentrations was obtained using the noncooperative McGhee−von Hippel model (*26*) which describes the non-sequence specific binding of a ligand to an infinite lattice of DNA binding sites. In this treatment, the dependence of L_b on D_t, L_t, and K was defined by

$$K\left(1 - n\frac{L_b}{D_t}\right)\left[\frac{1 - n\frac{L_b}{D_t}}{1 - (n-1)\frac{L_b}{D_t}}\right]^{n-1} - \frac{\frac{L_b}{D_t}}{L_t - L_b} = 0 \quad (2)$$

The value of L_b at given L_t and D_t values was determined using an adaptive grid refinement global optimization procedure (Loehle Enterprises, Naperville, IL) to locate the value of L_b which minimized the square of the above expression for each data point in the titration. Errors in the reported parameters are the standard deviations of the parameters obtained from three or more independent titrations.

Circular Dichroism. Circular dichroism data were collected on AVIV 62DS and Olis 1500 spectrometers. The CD instruments were calibrated using *d*-camphor-10-sulfonic acid. The molar CD per peptide bond was determined using standard procedures (*27*). All spectra were collected from 190 to 320 nm in 1 nm increments with an averaging time of at least 10 s/nm, and smoothed as described by Savitsky and Golay (*28*). Changes in CD spectra of DNA induced by the protein were measured by titration of poly(dGdC) in 0.01 M KH_2PO_4 and 0.025 M KCl at pH 7 (25 °C) with Sac7d in identical buffer.

Isothermal Titration Calorimetry. ITC was performed using VP-ITC (Microcal) and CSC 4200 (Calorimetry Sciences) calorimeters with overfilled cells from 5 to 90 °C (*29*). Buffer, DNA, and protein samples were degassed with gentle stirring under vacuum for 15 min. A typical titration consisted of 25−55 injections (5 μL each) of protein (0.3−

[1] Abbreviations: $\sigma(T)$, fractional progress of a reaction as a function of temperature; K_o, equilibrium constant for distortion of DNA in the absence of protein; A/A, double-alanine mutant V26A/M29A of Sac7d; F/F, double-phenylalanine mutant V26F/M29F of Sac7d; G/G, double-glycine mutant V26A/M29G of Sac7d; K_p, equilibrium constant for distortion of DNA in the Sac7d−DNA complex; L/L, double-leucine mutant V26L/M29L of Sac7d; M29A, single-alanine substitution of M29; Q_{max}, maximal intrinsic fluorescence quenching; T_m, midpoint temperature of a structural transition in the Sac7d−DNA complex; V26A, single-alanine substitution of Sac7d.

0.5 mM, in 0.01 M KH_2PO_4 and 0.025 M KCl at pH 7) into DNA (0.2−0.4 mM bases, in identical buffer) with a 300 rpm stirring rate.

ITC titrations were fit by nonlinear regression to the noncooperative McGhee−von Hippel model (*26*) to obtain the binding affinity (K), site size (n), binding enthalpy (H), and heat of dilution (or offset at completion of the titration). The heat observed with each injection is given by

$$q(i) = c\Delta H_b \Delta L_b(i) + h \quad (3)$$

where c is the cell volume, H_b is the molar heat of binding (per mole of protein), L_b is the change in concentration of the bound protein as a result of the ith injection, and h is the heat of dilution observed with each injection after saturation of the binding sites at the end of the titration (*29*, *30*). The change in concentration of bound L which contributes to the heat observed with injection i is given by

$$\Delta L_b(i) = L_b(i) - L_b(i-1) + 0.5\frac{\upsilon}{c}[L_b(i) + L_b(i-1)] \quad (4)$$

where υ is the volume of the injection and $L_b(i)$ and $L_b(i-1)$ refer to the concentrations of bound protein in the i and $i-1$ injections, respectively. The last term in eq 4 accounts for the heat produced by the volume that is ejected with each injection into an overfilled cell during the titration. The concentration of bound protein L_b following each injection was obtained from the noncooperative McGhee−von Hippel model (*26*) as described above for the fluorescence titrations. Errors in the parameters were defined by the standard deviations of the parameters obtained from fitting three or more titrations.

Differential Scanning Calorimetry. DSC data were collected on MicroCal Extended Range VP-DSC and Calorimetry Sciences Nano-II instruments with scans from 0 to 130 °C under a pressure of 3 atm as described previously (*29*). DSC samples typically contained 1 mg/mL (130 μM) protein in 0.01 M KH_2PO_4 and 0.025 M KCl at pH 7 and were degassed by being stirred under vacuum. Reversibility was monitored by repeated scans on the same sample, with the first scan terminated at the T_m. DSC data were fit by nonlinear regression to obtain both T_m and ΔH for the endotherms using in-house programs described elsewhere (*23*).

NMR Spectroscopy. $^1H-^{15}N$ HSQC spectra were collected on approximately 2.5 mM protein samples in 0.7 mL of a 90% H_2O/10% D_2O mixture at 30 °C using Varian INOVA 500 and 800 MHz NMR spectrometers with gradient selection of the ^{15}N magnetization and minimal perturbation of the water (*31*, *32*). ^1H chemical shifts were referenced to internal DSS, and ^{15}N chemical shifts were calculated from the relative frequencies (Ξ) (*33*) of ^1H (DSS) and ^{15}N (liquid ammonia) chemical shift references (*34*). Sac7d $^1H-^{15}N$ HSQC peak assignments have been presented previously (*22*). Mutant protein HSQC assignments were made by comparison to the Sac7d data and corroborated with three-dimensional $^1H-^{15}N$ TOCSY-HSQC.

RESULTS

Intercalating Residue Mutations. Intercalating residues V26 and M29 were individually substituted by site-directed mutagenesis to obtain the V26A and M29A recombinant proteins. In addition, substitution of both intercalating residues with alanine, leucine, phenyalanine, tryptophan, and glycine led to the double-mutant proteins termed A/A (representing V26A/M29A), L/L, F/F, W/W, and G/G, respectively. An initial comparison of DNA binding by the A/A double mutant and Sac7d has been described elsewhere (*18*). Two triple mutants, W24G/V26G/M29G and W24A/V26A/M29A, were also created; however, these proteins and double mutant W/W displayed weak DNA binding and were not further characterized.

Effect of Mutations on Protein Structure and Stability. The mutations described here led to negligible changes in the CD spectrum of Sac7d. Secondary structure content calculated using CDPro (*35*) indicated that Sac7d contained 22.1 ± 1.9% α-helix, 35.1 ± 1.4% β-sheet, 15.9 ± 1.5% β-turn, and 26.8 ± 4.1% other secondary structure, and similar values were obtained for all of the single and double mutants. $^1H-^{15}N$ HSQC NMR spectra also indicated that none of the mutations resulted in major backbone disruption. Only small changes in HSQC peak positions were observed for residues in the vicinity of the substituted residues.

All of the Sac7d mutations described here resulted in a decrease in the thermal stability of the protein under the conditions used for DNA binding experiments. Increased surface hydrophobicity in double mutants F/F and L/L resulted in T_m values of 87 and 88 °C, respectively (in 0.10 M KH_2PO_4 and 0.025 M KCl at pH 7). This represents a small decrease relative to that of native Sac7d which unfolds with a T_m of 90.7 °C under the same conditions. A reduction in surface hydrophobicity in V26A, M29A, and A/A also slightly lowered the stability of the protein with T_m values of 89, 84, and 81 °C, respectively. Substitution of glycine at both positions resulted in the lowest stability of the double mutant proteins with a T_m of 76 °C. Triple alanine and glycine mutations (W24A/V26A/M29A and W24G/V26G/M29G, respectively) both resulted in large decreases in stability with T_m values of 69 and 67 °C, respectively. Most importantly, the thermal stabilities of all of the mutant proteins were sufficient to perform DNA binding studies over an unusually wide range of temperatures that exceeded that commonly available with mesophile proteins. The high thermal stability of Sac7d and the mutant proteins eliminated the need to correct for unfolding over the temperature range from 0 to 65 °C.

Fluorescence Titrations. Sac7d contains a single tryptophan (W24) which is solvent-exposed on the protein surface adjacent to the intercalating residues (Figure 1). DNA binding results in 80−90% quenching of the intrinsic tryptophan fluorescence (*23*). Reverse titrations followed by fluorescence have been used to characterize binding of the Sac7d mutant proteins by fitting to the noncooperative McGhee−von Hippel model (*24*). The high signal-to-noise ratio of the fluorescence titration data made it the preferred method for defining both binding affinity and DNA binding site size. The magnitude of maximal quenching also served as a sensitive indicator of the environment of the tryptophan buried at the DNA−protein interface.

Truncation of V26 and M29 lowered the affinity of Sac7d for DNA. The single V26A substitution resulted in a 5-fold reduction in affinity (in 0.01 M KH_2PO_4 and 0.025 M KCl at pH 7 and 25 °C), while the M29A mutation led to an

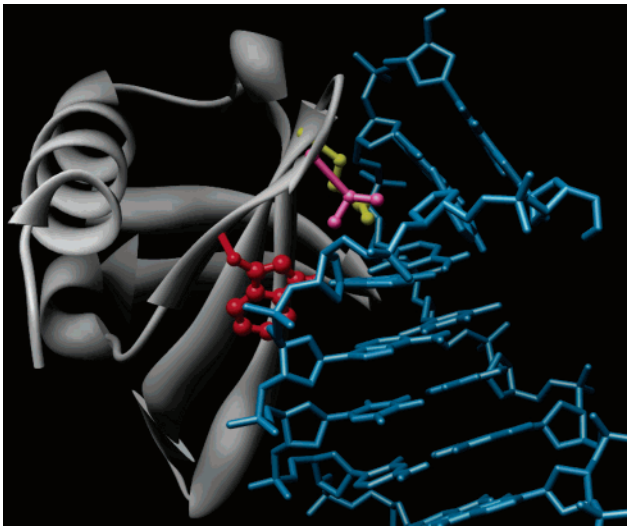

FIGURE 1: Kinking of DNA by Sac7d is shown in the X-ray crystal structure (PDB entry 1azp) of Sac7d (gray) bound to duplex GCGATCGC (blue). The intercalating side chains from V26 (magenta) and M29 (yellow) are shown inserted at the kink between the second and third base pairs with a roll angle of 66°. The single tryptophan (W24) in Sac7d is shown (red) on the surface of the three-stranded β-sheet which inserts into the DNA minor groove that is widened as a result of unwinding and bending of the DNA.

only ~2-fold reduction (Table 1). Within experimental error, the binding site size was essentially unchanged by both the single- and double-alanine substitutions. Significant maximal quenching was observed at 25 °C, with Q_{max} reduced by ~15% for the single mutations, compared to ~30% for the double A/A mutant. The double G/G mutant showed a binding affinity similar to that observed for A/A, and the binding site size was slightly smaller. Notably, the maximal quenching observed for the double-glycine mutant was only 22% at 25 °C, the lowest observed for any of the proteins.

Increasing the hydrophobicity of the intercalating side chains in L/L and F/F resulted in an increase in the affinity for poly(dGdC), with the affinity for the double-phenylalanine mutant being more than 5 times greater than that of native Sac7d at 25 °C. The maximal fluorescence quenching and binding site sizes for L/L− and F/F−DNA complexes were similar to those observed for Sac7d. This was taken as indirect evidence that the structures of the DNA complexes with L/L and F/F were similar to that observed for Sac7d. W/W showed very weak binding, indicating that the larger size of the tryptophan was detrimental.

Temperature Dependence of Binding Affinity, Site Size, and Fluorescence Quenching. The high thermal stability of the Sac7d mutant proteins as well as 1000 bp poly(dGdC) permitted an investigation of the temperature dependence of binding from 5 to 85 °C using fluorescence titrations. DNA binding affinities of all of the mutant proteins increased with an increase in temperature, similar to that observed for Sac7d (Figure 2). An increase in affinity with temperature is indicative of a positive heat of binding and is consistent with observations on many proteins which bend DNA (*18*). The increase observed here indicates an enthalpy of binding of ~5 kcal/mol. A direct (and more accurate) determination of the binding enthalpies for each protein was obtained using ITC (see below).

The DNA binding site size for all of the proteins was essentially the same (viz. 3.3 ± 0.3 bp) and independent of temperature (Figure 3). Conservation of site size indicates that altering the intercalation side chains and the changing temperature do not significantly change the binding mode and orientation of the protein on the DNA. This is confirmed by the crystal structures of DNA complexes with V26A, M29A, and V26A/M29A (A. H.-J. Wang, personal communication).

In contrast, the temperature dependence of maximal fluorescence quenching varied with the size and hydrophobicity of the substituted residues (Figure 4). The Q_{max} for L/L and F/F was essentially independent of temperature up to 60 °C, similar to that observed for native Sac7d. These proteins also showed the highest Q_{max} values (viz. 80−90%). V26A, M29A, and A/A showed a significant temperature dependence for Q_{max}, with a clear decrease occurring at lower temperatures. The largest change with decreasing temperature was observed for A/A (Q_{max} < 40% at 5 °C), followed by V26A (46%) and M29A (55%). The upper limit for Q_{max} at high temperatures for these proteins approached the temperature-independent value observed for L/L, F/F, and Sac7d. The temperature dependence of Q_{max} indicates that the structure of the DNA complex changes with temperature, and approaches that observed for Sac7d at high temperatures. The Q_{max} for the G/G−DNA complex was significantly reduced compared to those of the other proteins.

The magnitude of quenching of the intrinsic tryptophan fluorescence of Sac7d by DNA reflects the proximity of W24 to the sugar−phosphate backbone and possibly hydrogen bonding to a nucleotide base indicated by the crystal structures of Sac7d−DNA complexes (*12*, *36*). The temperature dependence of Q_{max} therefore indicates a temperature-dependent structural change at the protein−DNA interface. The temperature dependences for the A/A−, V26A−, and M29A−DNA complexes were fit to a two-state equilibrium model where the observed Q_{max} was a weighted sum of the upper and lower temperature limits, with each weighted by the relative populations of two species:

$$Q_{max}^{obs} = [1 - \alpha(T)]Q_{max}^{lower} + \alpha(T)Q_{max}^{upper} \quad (5)$$

where $\alpha(T)$ is the fractional population of the upper temperature form and is given by

$$\alpha(T) = K(T)/[1 + K(T)] \quad (6)$$

where

$$K(T) = e^{-\Delta G(T)/RT} \quad (7)$$

$$\Delta G(T) = \frac{\Delta H(T_m - T)}{T_m} \quad (8)$$

where T_m is the midpoint temperature of the structural transition in the protein−DNA complex.

ΔC_p was not reliably defined by the temperature dependence of the spectroscopic signal, and therefore, it was set to zero. The lower limit of Q_{max} was also not defined well by the data, but the Q_{max} values observed for G/G indicate that it can be expected to fall between 0 and 0.2. The influence of the lower fluorescence limit Q_{max}^{lower} on the fitted values for T_m and ΔH was investigated by constraining Q_{max}^{lower} to 0.0 (i.e., no fluorescence change upon binding),

Table 1: Parameters Characterizing Binding of Sac7d and Mutant Proteins to Poly(dGdC)[a]

protein	*n* (bp)	Q_{max}	*K* (M)	ΔG (kcal/mol)	ΔH (kcal/mol)	ΔC_p (cal deg^{-1} mol^{-1}) low[b]	ΔC_p (cal deg^{-1} mol^{-1}) high
Sac7d	3.5 ± 0.4	0.88 ± 0.01	(3.5 ± 1.6) × 10^6	−8.9 ± 0.3	9.2 ± 1.4	−	−184 ± 13 (5−60)
A/A	3.9 ± 0.4	0.63 ± 0.07	(0.36 ± 0.21) × 10^6	−7.4 ± 0.5	8.3 ± 1.0	+170 ± 24 (5−30)	−271 ± 45 (45−60)
V26A	3.75 ± 0.2	0.75 ± 0.03	(0.63 ± 0.23) × 10^6	−7.9 ± 0.1	9.2 ± 1.1	+141 ± 46 (5−15)	−129 ± 14 (20−65)
M29A	4.2 ± 0.3	0.77 ± 0.03	(2.2 ± 1.9) × 10^6	−8.5 ± 0.4	11.5 ± 0.8	+190 ± 72 (5−15)	−194 ± 12 (25−65)
L/L	3.7 ± 0.2	0.83 ± 0.01	(15.0 ± 3.2) × 10^6	−9.8 ± 0.1	11.9 ± 1.2	−	−217 ± 21 (10−50)
F/F	3.7 ± 0.3	0.83 ± 0.01	(19.0 ± 0.6) × 10^6	−9.9 ± 0.02	9.7 ± 0.3	−	−178 ± 7 (10−50)
G/G	2.9 ± 0.1	0.22 ± 0.01	(0.46 ± 0.01) × 10^6	−7.7 ± 0.01	1.1 ± 0.5	−	−23 ± 13 (10−40)

[a] Binding constants (*K*), site sizes (*n*, in base pairs), and maximal quenching (Q_{max}) in 0.01 M KH_2PO_4 and 0.025 M KCl at pH 7 and 25 °C were measured by fluorescence titrations as described in Experimental Procedures. Heats of binding (ΔH) were measured by ITC under similar conditions. Values for *K*, *n*, and Q_{max} are averages of at least three data sets. ΔH at 25 °C (and the associated error) was obtained by regression of the temperature dependence of the heat of binding. Errors in parentheses are standard deviations. Binding free energies were calculated from binding constants using $\Delta G = -RT \ln K$. The ΔC_p of binding (and the associated error) was obtained by regression of the temperature dependence of the heat of binding. [b] For V26A, M29A, and A/A, the apparent ΔC_p indicated by the temperature dependence of ΔH is given for both the low-temperature range where ΔC_p is positive and the higher temperature range where ΔC_p is negative.

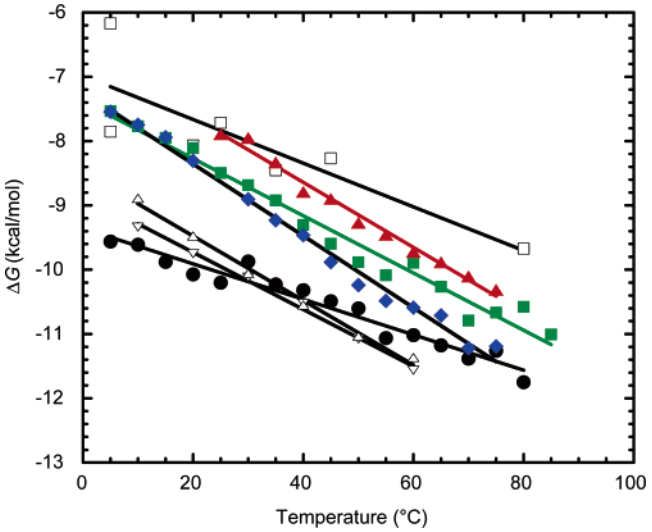

FIGURE 2: Temperature dependence of the free energy of DNA binding by Sac7d and mutant proteins. The binding free energies were determined from the binding affinities determined from reverse titrations of the protein with poly(dGdC) in 0.01 M KH_2PO_4 and 0.025 M KCl at pH 7. The quenching of the intrinsic tryptophan fluorescence was fit by nonlinear regression to the noncooperative McGhee−von Hippel model: Sac7d (●), V26A (green ■), M29A (blue ◆), A/A (red ▲), L/L (△), F/F (▽), and G/G (□).

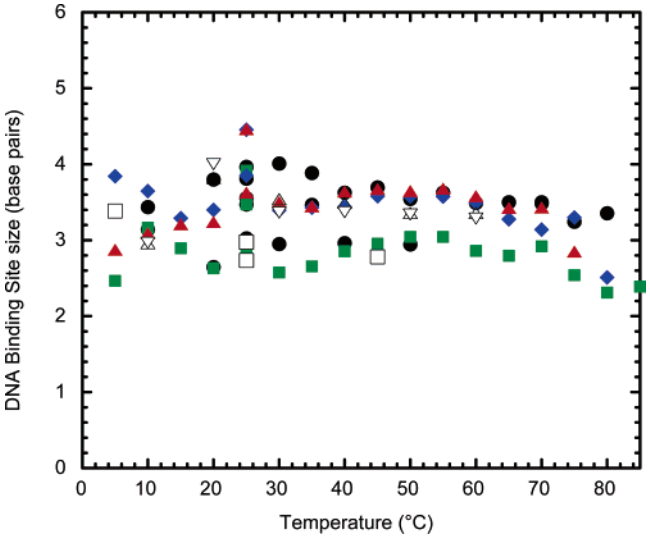

FIGURE 3: Temperature dependence of the DNA binding site size occluded by Sac7d and mutant proteins. Site sizes were obtained from reverse titrations of the protein with poly(dGdC) in 0.01 M KH_2PO_4 and 0.025 M KCl at pH 7. The quenching of the intrinsic tryptophan fluorescence of the protein titrated with poly(dGdC) was fit by nonlinear regression to the noncooperative McGhee−von Hippel model. Symbols are the same as those in Figure 2.

0.1, and 0.2 (the value observed for G/G at 25 °C) in a nonlinear fit of the M29A, V26A, and A/A data to eq 5. The fitted value for ΔH was relatively insensitive to the constrained lower limit value, varying by no more than 3 kcal/mol if Q_{max}^{lower} varied from 0.0 to 0.2. The fitted value for T_m was much more sensitive to the lower limit constraint and varied by up to 7 °C if the lower limit was varied from 0.0 to 0.2. The estimated error in ΔH was therefore ±3 kcal/mol, and that for T_m was ±7 °C. Assuming a Q_{max}^{lower} of 0.2, the ΔH values for the three proteins were seen to be approximately 17.5 kcal/mol, and the T_m values varied from 1.6 °C (M29A) to 5.8 °C (V26A) and 14.5 °C (A/A).

Changes in DNA Circular Dichroism with Protein Binding. The CD spectrum of poly(dGdC) was significantly altered by the binding of Sac7d and the majority of the mutant proteins. A representative series of spectra are shown in Figure 5 with the titration of poly(dGdC) with V26A. At wavelengths above 250 nm, contributions from DNA dominate the CD spectrum of the protein−DNA complex, and spectral changes in a forward titration of the protein into DNA attain a plateau consistent with saturation of the DNA. The presence of an isodichroic point at 272 nm indicates that the change associated with binding reflects a two-state transition in the DNA. Notably, the 4-fold increase in CD in the near UV (285 nm) is indicative of distortion induced in the DNA by protein binding, and is consistent with DNA unwinding and bending as observed in the X-ray crystal structures of Sac7d− and Sso7d−DNA complexes (*12*, *36*, *37*). Therefore, changes in the CD at 285 nm are interpreted as distortions in DNA structure induced by protein binding.

The magnitude of the near-UV CD change at 20 °C depended on the size and hydrophobicity of the residues substituted for V26 and M29 (Figure 6). Most importantly, the relative magnitudes of the CD change induced by each mutant protein were similar to those observed for the maximal fluorescence change. The largest changes were observed for L/L and F/F, and these were similar to that observed for native Sac7d. Titration with G/G had a negligible effect on the DNA CD spectrum at 285 nm and

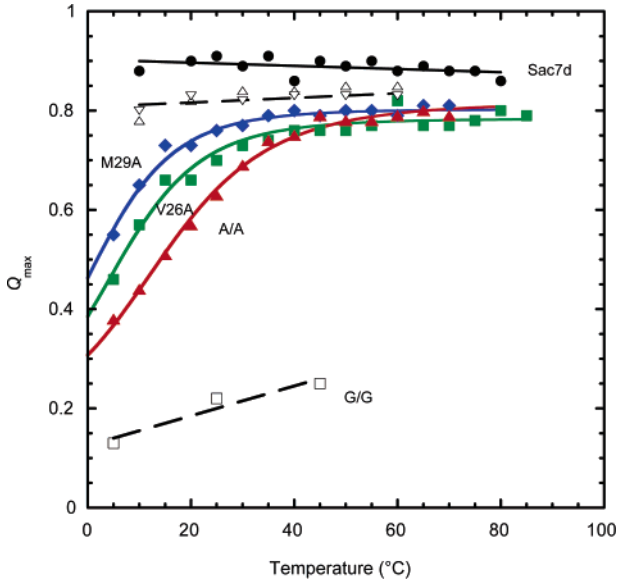

FIGURE 4: Temperature dependence of the maximal fluorescence quenching obtained in reverse titrations of Sac7d and mutant proteins with poly(dGdC) in 0.01 M KH_2PO_4 and 0.025 M KCl at pH 7. Protein concentrations ranged from 1 to 5 μM. Symbols are the same as those in Figure 2.

20 °C, and that observed for A/A was only slightly larger. Both single-alanine substitutions led to a larger change at 20 °C that was intermediate between those observed for A/A and native Sac7d.

As observed for Q_{max}, a significant temperature dependence was observed for the CD intensities for V26A−, M29A−, and A/A−DNA complexes at 285 nm (Figure 6). The change in CD for DNA complexes with these proteins reached a plateau at high temperatures at a value approaching that observed for native Sac7d. The CD change induced by A/A was significantly less than observed for either single mutant, and reached a plateau at a high temperature which was only ~40% of that induced by native Sac7d. Again, similar to that observed for Q_{max}, little temperature dependence was observed for the L/L− and F/F−DNA complexes. The G/G mutant induced essentially no change in the CD spectrum of DNA from 5 to 80 °C.

The temperature dependence of the change in CD observed for V26A, M29A, and A/A was fit to a two-state equilibrium model similar to that described above for the fluorescence data (eq 5) with ΔC_p for the transition set to zero. The upper CD limit was included as a fitting parameter specific for each protein. The lower CD limit was constrained to that observed for the G/G data (i.e., no change relative to that of free DNA). As observed for the fluorescence data, varying the value of the constrained lower CD limit had a larger effect on the fitted T_m than on ΔH. The estimated error in T_m was on the order of 5 °C, while the error in ΔH was estimated to be 3 kcal/mol.

Although the error in the T_m values derived from the CD data is significant given the lack of definition of the lower CD limit, the temperature dependence of the data indicates that the T_m for the M29A−DNA (1.4 °C) complex was lower than that for the V26A−DNA complex (8.4 °C), and the T_m for the A/A−DNA complex occurred at the highest temperature (19 °C). The mean ΔH for the transition in the protein−DNA complexes indicated by the CD was 12.2 ± 2.2 kcal/mol. Given the estimated error resulting from the lack of definition of the lower limits, the thermodynamic parameters derived from the temperature dependence of the CD are in reasonable agreement with those derived from the fluorescence data.

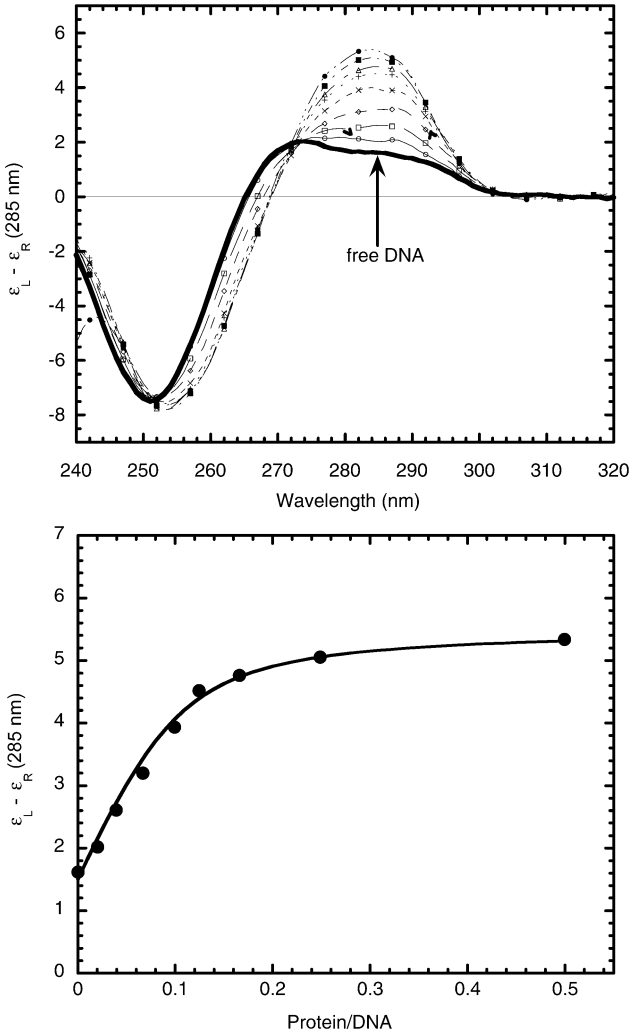

FIGURE 5: Change in the near-UV circular dichroism spectrum of poly(dGdC) due to binding of V26A Sac7d. Poly(dGdC) (top panel) was titrated with increasing concentrations of protein in 0.01 M KH_2PO_4 and 0.025 M KCl at pH 7 and 25 °C [71 μM DNA; protein/DNA ratios of 0.0 (thick curve), 0.02, 0.04, 0.067, 0.1, 0.125, 0.166, 0.25, and 0.5]. Saturation of the DNA is demonstrated by the dependence of the near-UV CD at 285 nm on the protein/DNA ratio in the bottom panel.

Calorimetric Measurement of the Enthalpy and ΔC_p of DNA Binding. Direct measurement of the heat of DNA binding by the mutant proteins was obtained by ITC. Data were fit using the noncooperative McGhee−von Hippel model (*26*) for binding to an infinite lattice to obtain the binding enthalpy (Table 1).[2] All of the proteins demonstrated a positive, unfavorable enthalpy of binding at 25 °C in 0.01 M KH_2PO_4 and 0.025 M KCl at pH 7. As observed for most

[2] Nonlinear regression of ITC data provided site sizes and affinities for each protein which were generally consistent with those determined by fluorescence titrations. Because of the greater signal-to-noise ratio in the fluorescence data, site sizes and binding affinities extracted from fluorescence titrations were considered to be more accurate than those from ITC, and the ITC measurements were used to obtain heats of binding.

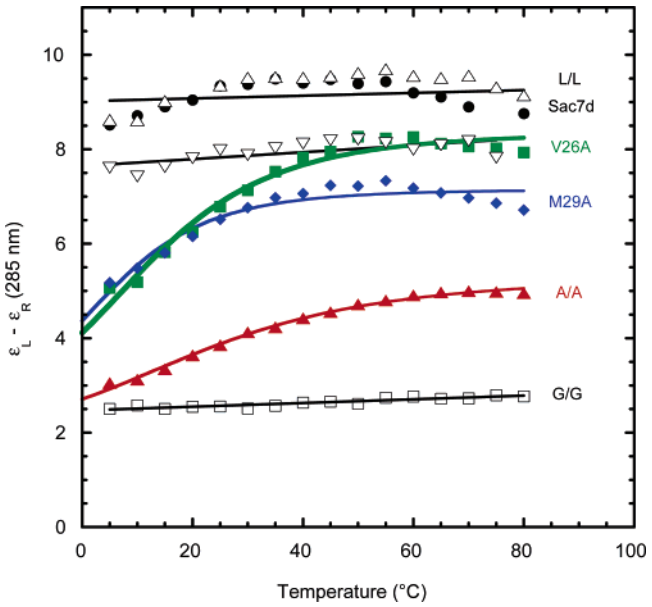

FIGURE 6: Temperature dependence of the maximal CD change observed in a forward titration of poly(dGdC) Sac7d and mutant proteins. Titrations were performed in 0.01 M KH_2PO_4 and 0.025 M KCl at pH 7. Initial protein concentrations were approximately 40 μM. Symbols are the same as those in Figure 2.

DNA binding proteins, the enthalpy was temperature-dependent (Figure 7) and approached zero around 70−75 °C. An exothermic contribution at high temperatures (above 60 °C) was previously shown for native Sac7d and A/A to be due to DNA-induced refolding of the protein near the protein unfolding T_m.

For F/F and L/L, the temperature dependence of the enthalpy was linear below 60 °C with a ΔC_p similar to that observed for native Sac7d (Table 1). The ΔC_p observed for Sac7d has been previously shown to be in good agreement with that expected from the change in accessible surface area based on the crystal structure of the complex (*18*). The enthalpy of binding for L/L was slightly (3 kcal/mol) greater than that observed for Sac7d at any temperature, while that for F/F was more similar to that for Sac7d.

Most importantly, the temperature dependence of the binding enthalpy for V26A, M29A, and A/A deviated significantly from that observed for native Sac7d at low temperatures. Similar to that previously described for A/A, the temperature dependence of the heat of DNA binding by V26A and M29A showed the usual negative heat capacity of binding at high temperatures (i.e., near 50 °C), but in the lower temperature range (e.g., 0−20 °C), a downward curvature in the ΔH versus T plot led to an unusual positive ΔC_p. The temperature range for the positive ΔC_p varied with the mutation, with M29A and V26A showing a positive ΔC_p from 5 to ~20 °C, and A/A from 5 to ~40 °C. The significant negative heat capacity of binding above 65 °C was attributed to protein refolding induced by binding and was not further considered.

A Positive ΔC_p of DNA Binding Can Be Explained by DNA Distortion. The temperature ranges observed for the positive heat capacity of binding for V26A, M29A, and A/A were in good agreement with those observed for the temperature dependence of Q_{max} and CD. This indicates that the unusual positive heat capacity may result from a temperature-dependent structural transition in the DNA complex (*18*).

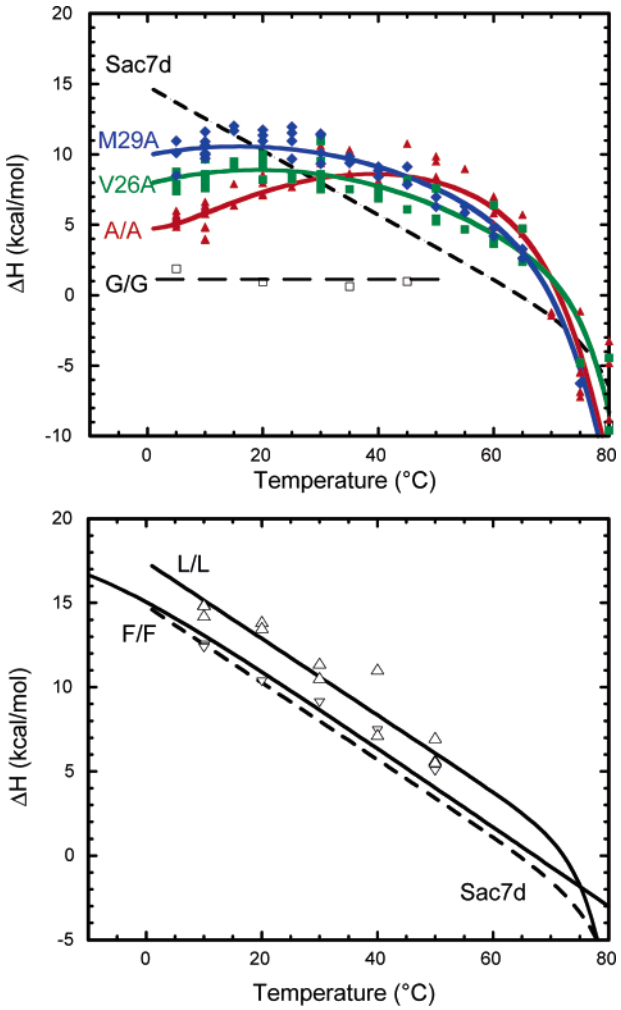

FIGURE 7: Temperature dependence of the molar heat of binding of Sac7d and mutant proteins to poly(dGdC) in 0.01 M KH_2PO_4 and 0.025 M KCl at pH 7. Proteins with truncated intercalating residues are shown in the top panel, and substitutions resulting in increased size and hydrophobicity of the intercalating residue are shown in the bottom panel. Symbols are the same as those in Figure 2.

Other contributions to a positive ΔC_p have been discussed elsewhere and eliminated in favor of a structural transition in the protein−DNA complex (*18*).

The linkage of a temperature-dependent structural transition in DNA to protein binding can be described by the scheme shown in Figure 8, where DNA is shown to exist in linear (D_l) and distorted (D_d) states, with the protein (P) capable of binding to both. Given the persistence length and stability of poly(dGdC), it can be assumed that in the absence of the protein, the DNA exists predominantly as linear undistorted B-DNA over the entire temperature range studied here, and therefore, $K_o \ll 1$. The distortion of the DNA in the protein−DNA complex is characterized by an equilibrium constant K_p with a midpoint temperature T_m, as well as enthalpy and heat capacity changes, ΔH_p and $\Delta C_{p,p}$, respectively. In the vicinity of the T_m, K_p will vary significantly with temperature and the progress, $\alpha(T)$, of the distortion reaction is given by

$$\alpha(T) = \frac{K_p}{1 + K_p} \qquad (9)$$

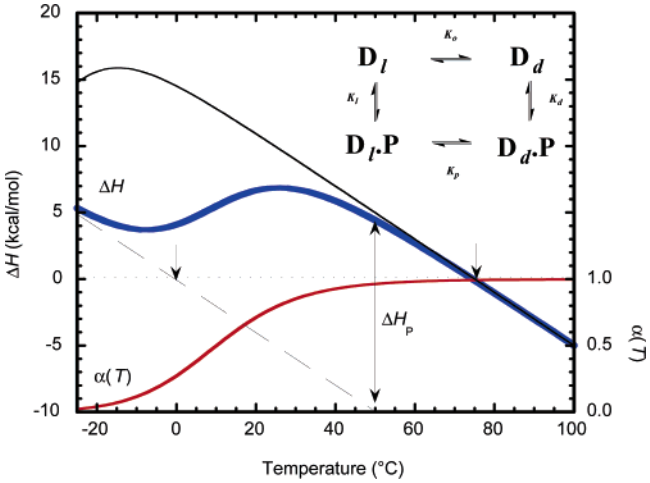

FIGURE 8: Effect of a temperature-dependent structural transition in a protein−DNA complex on the enthalpy of binding. The DNA is assumed to exist in two states (inset): a linear B-DNA form (D_l) and a distorted bent form (D_d). The protein can bind to both forms, but it is assumed that the linear form predominates in the absence of protein. The effect of an endothermic structural transition on the temperature dependence of the observed binding enthalpy (thick blue curve) is shown where the transition occurs in the temperature range being studied. The T_m for the distortion in the complex is 10 °C with a ΔH_p of 15 kcal/mol (the ΔC_p for the transition is set to 0). Protein binding to D_l is characterized by a ΔC_p of −200 cal deg^{-1} mol^{-1} and a ΔH of −5 kcal/mol at 25 °C [values consistent with the energetics of DNA binding without bending (*18*)]. In the absence of distortion, the temperature dependence of the binding enthalpy would follow the dashed curve and the temperature of maximal binding affinity would occur at 0 °C where $\Delta H = 0$ (indicated by the arrow on the left side). In the presence of distortion, the temperature dependence of the binding heat increases sigmoidally by ΔH_p (double arrow) and the temperature of maximal binding affinity in the presence of bending is shifted to 75 °C (arrow on the right side). The sigmoidal increase in the enthalpy of binding coincides with the progress curve (red) for the transition which would be observed by spectroscopic probes sensitive to the transition (e.g., fluorescence and CD).

where the temperature dependence of K_p is defined by exp(−$\Delta G_p/RT$), and

$$\Delta G_p(T) = \Delta H_p\left(\frac{T_m - T}{T}\right) - \Delta C_{p,p}(T_m - T) + T\Delta C_{p,p}\ln\left(\frac{T_m}{T}\right) \quad (10)$$

The overall enthalpy of binding is given by (*18*)

$$\Delta H = \Delta H_l + \left(\frac{K_p}{1+K_p}\right)\Delta H_p - \left(\frac{K_o}{1+K_o}\right)\Delta H_o \quad (11)$$

The first term on the right side of eq 11 is the enthalpy of binding to linear, undistorted DNA, and the second term is an additional contribution from the distortion reaction weighted by the extent of the reaction (eq 9). The third term arises from temperature-dependent changes in the free DNA, and is ignored here given the stability and persistence length of 1000 bp DNA. A similar term would arise if a structural change occurred in the free protein, and thus is also eliminated from consideration for data below 60 °C. Taking the derivative of ΔH as a function of temperature (and ignoring contributions from K_o), we obtain an expression for the change in heat capacity associated with binding:

$$\Delta C_p = \Delta C_{p,l} + \left[\frac{K_p}{(1+K_p)^2}\right]\frac{\Delta H_p^2}{RT^2} \quad (12)$$

where the first term on the right side is the change in heat capacity resulting from binding to D_l and the second term represents an excess ΔC_p arising from driving the distortion reaction. A third term would arise if contributions from transitions in the free protein and/or free DNA contributed to binding, and this term will always make a negative contribution (*18*).

Equation 12 demonstrates that a contribution to the binding ΔC_p from a temperature-dependent structural change in the protein−DNA complex will always be positive. In addition, the contribution only occurs in the vicinity of the T_m of the transition. The temperature dependence of the heat of binding (eq 11) contains a sigmoidal contribution defined by the progress of the distortion reaction. A temperature-dependent structural change indicated by a sigmoidal temperature dependence of a spectroscopic signal defined by $\alpha(T)$ (eq 9) coincides with an increase in the ΔH of binding (Figure 8).

The linkage model provides the most straightforward explanation of not just the observed positive heat capacity. In addition, it explains why those proteins which do not exhibit a positive heat capacity also do not show a temperature-dependent change in CD and Q_{max} over the same temperature range. Only DNA complexes with A/A, V26A, and M29A indicate a temperature-dependent structural transition in the complex with a T_m that ranges from ∼2 to 20 °C (Table 2), and only these proteins also demonstrate an increase in the heat of binding over the same temperature range (Figure 9).

A more quantitative comparison of the temperature dependence of the binding enthalpy observed for V26A, M29A, and A/A to the temperature dependence of the spectroscopic parameters can be gained from fitting the enthalpy data to obtain T_m and ΔH values for the three mutant proteins. The temperature dependence of the binding enthalpy was fit to eq 11 with K_o set to 0 (i.e., assuming no temperature-dependent contributions from free DNA). As with the CD and fluorescence data, the lower limit of the temperature dependence of the binding enthalpy is not defined by the data. For the purposes of an initial fit of the data, the enthalpy of binding to undistorted DNA (ΔH_l) was set to 0 kcal/mol at 0 °C, which approximates the mean binding heat for proteins binding to DNA without bending [see Figure 9A in Peters et al. (*18*)], and the ΔC_p of binding was constrained to that observed for the native Sac7d (−236 cal deg^{-1} mol^{-1}). The fitted curves are overlaid on the data in Figure 9, and the values obtained for T_m and ΔH for each protein are given in Table 2.

DISCUSSION

We have shown that the temperature dependence of the DNA binding enthalpy for various Sac7d intercalation side chain mutants is correlated with the temperature dependence of spectral changes associated with formation of the protein−DNA complex. The native and mutant proteins can be grouped into two classes. The first class contains four proteins (native Sac7d, L/L, F/F, and G/G) which displayed a linear temperature dependence below 60 °C for the heat

Table 2: Thermodynamic Parameters Characterizing the $D_l \rightarrow D_b$ Transition As Reflected in the Temperature Dependence of Maximal Protein Fluorescence Quenching (Q_{max}), DNA Circular Dichroism, and Binding Enthalpies Observed for Binding of Poly(dGdC) to Sac7d Mutant Proteins[a]

	protein Q_{max}		DNA CD		ITC	
protein	T_m (°C)	ΔH (kcal/mol)	T_m (°C)	ΔH (kcal/mol)	T_m (°C)	ΔH (kcal/mol)
A/A	14.5 ± 0.4	15.8 ± 0.8	19.0 ± 0.8	10.0 ± 0.5	16.5 ± 1.2	13.1 ± 1.2
V26A	5.8 ± 0.9	18.2 ± 2.0	8.4 ± 1.0	12.2 ± 1.4	6.8 ± 1.2	11.1 ± 1.6
M29A	1.6 ± 1.0	18.7 ± 2.3	1.4 ± 1.8	14.4 ± 2.7	2.6 ± 0.7	16.7 ± 1.9

[a] Data collected in 0.01 M KH_2PO_4 and 0.025 M KCl at pH 7. Fluorescence data were fit to eq 7 by nonlinear regression with the lower limit of Q_{max} constrained to 0.2 for all proteins. The CD data were fit similarly with the lower limit constrained to 2.0 for all proteins. The ITC data were fit to eq 11 with the lower limit defined as described in the text for all proteins.

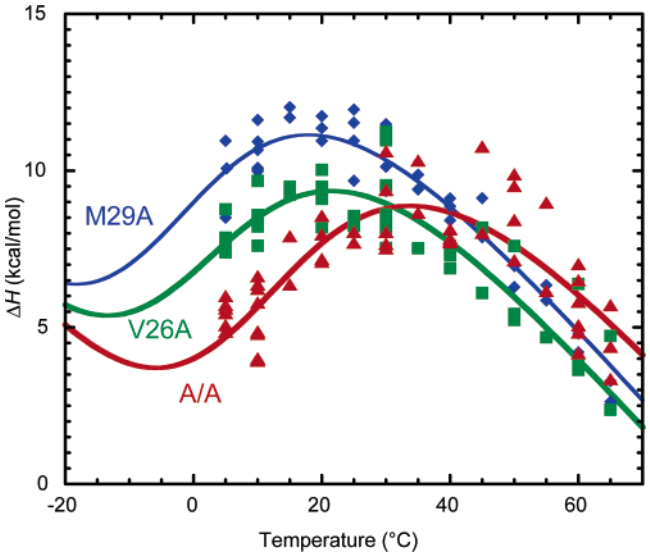

FIGURE 9: Fitting of the temperature dependence of the poly(dGdC) binding enthalpy of V26A, M29A, and A/A. Data collected above 65 °C reflect an induced refolding of the protein as the T_m of the protein is approached and are excluded. The data were fit to obtain T_m and ΔH values for A/A, V26A, and M29A as described in the text.

of binding as well as changes in DNA CD and protein Q_{max} with binding. For three of these proteins (Sac7d, L/L, and F/F), the binding ΔH and the change in CD and Q_{max} were near the maximal changes observed at all temperatures and appeared to define an upper limit for the observed parameters. In contrast, the CD, Q_{max}, and ΔH values for G/G were at the lower range of values observed for all the proteins and appeared to define a lower limit.

The second class of mutant proteins (V26A, M29A, and A/A) showed a nonlinear temperature dependence below 60 °C for the binding ΔH as well as changes in CD and Q_{max} resulting from DNA binding. The nonlinearity for the temperature dependence of the three parameters occurred over the same temperature range for each mutant, with values falling between the upper and lower limits defined by the first class. All of the data are consistent with an endothermic structural transition in the complex with the apparent midpoint temperatures dependent on the intercalating side chains. The midpoint temperatures defined by the binding heats of A/A, V26A, and M29A (viz. 16.5, 6.8, and 2.6 °C, respectively) were in good agreement with those obtained for Q_{max} (viz. 14.5, 5.8, and 1.6 °C, respectively) as well as for changes in the CD of DNA (viz. 19.0, 8.4, and 1.4 °C, respectively). The level of agreement between the midpoint temperatures determined by the three data sets is good, with differences (standard deviations of 2.2, 1.3, and 0.6 °C, respectively) within the error of the fitted parameters and attributed to the lack of data for accurately defining the lower limits or baselines for all three data sets.

The temperature dependence of the CD and Q_{max} data for proteins in the second class indicate mean van't Hoff ΔH values for the structural transition of 12.2 and 17.6 kcal/mol, respectively. This compares favorably with the average ΔH obtained from the temperature dependence of the binding heat, i.e., 13.6 kcal/mol. Thus, the temperature dependencies of the CD, Q_{max}, and heat of binding together indicate that the structural transition observed in DNA complexes with mutant proteins V26A, M29A, and A/A increases the enthalpy of binding by ~14.4 ± 3 kcal/mol.

It is reasonable to expect that DNA complexes with proteins in the first class also undergo a thermotropic transition similar to that observed for V26A, M29A, and A/A except that the midpoints of the transitions are outside the experimentally accessible temperature range. Since the observed CD, Q_{max}, and enthalpy values for DNA complexes of Sac7d, F/F, and L/L define the upper limit for these parameters as a function of temperature, the transition temperature for these proteins is expected to be below 0 °C, as indicated by the top curve in Figure 8. The unfavorable enthalpy observed for DNA binding to these proteins is therefore attributed to a structural transition which is similar to that observed for proteins in the second class.

The van't Hoff equation $[\partial R \ln K/d(1/T) = -\Delta H]$ stipulates that maximal binding affinity occurs at the temperature where ΔH passes through zero (i.e., T_H). As shown graphically in Figure 8, an additional contribution to the enthalpy of binding of 15 kcal/mol can lead to a considerable increase in the T_H. Clearly, distortion of DNA can result in significant perturbation of the temperature dependence of protein−DNA affinity. Many mesophile proteins distort DNA and bind with an unfavorable enthalpy of binding at 25 °C. The temperature of maximal DNA affinity for these proteins therefore cannot coincide with the temperature at which the protein normally functions in vivo. The temperature of maximal affinity may not have any biological relevance since what matters most is that the binding affinity is appropriate for the function at the physiological growth temperature. However, DNA distortion may be an effective mechanism in hyperthermophiles for increasing the stability of protein−DNA complexes at high temperatures.

As indicated above, the large increase in near-UV CD observed in poly(dGdC) upon Sac7d binding is consistent with unwinding and bending of the DNA which is observed in the crystal structure of the complex. This is supported by the agreement between the magnitudes of the changes in

DNA CD induced by A/A, V26A, and M29A and the relative magnitudes of the roll angles observed in the crystal structures of DNA complexes with these proteins (S. Su and A. H.-J. Wang, personal communication). We therefore propose that the change in CD is proportional to the bend angle induced in the DNA, and the temperature dependence in the CD of DNA bound to V26A, M29A, and A/A is the result of a temperature-dependent bending of the DNA in these complexes. We note that the energetics of the $D_lP \rightarrow D_dP$ reaction cannot represent simply the bending of DNA, since any adjustment in the DNA structure must be associated with changes at the interface in addition to bending. The initial binding reaction characterized by K_l most likely establishes many of the electrostatic interactions which occur in the final complex following bending. Enhanced intermolecular interactions are expected to accompany intercalation and bending, including improved hydrophobic and H-bonding interactions. The net contribution of these to the enthalpy of binding should be near zero or slightly favorable (*38*). Therefore, the unfavorable increase in enthalpy associated with the distortion reaction is expected to represent a lower limit for the enthalpy of bending.

CONCLUSIONS

The intercalating side chains of V26 and M29 play a key role in defining the energetics of Sac7d binding and bending of DNA. Mutations of the intercalating residues have been described which have varying effects on the energetics of binding as well as the structure of the protein−DNA complex. A subset of these mutations enables the observation of a thermotropic transition in the protein−DNA complex which is reflected by similar temperature dependences for both the heat of binding and spectroscopic signals associated with the structure of the complex. We conclude that the transitions observed by calorimetric and spectroscopic methods are the same. The data support our previous proposal that the positive ΔC_p for binding of A/A to DNA was due to a temperature-dependent bending of DNA in the complex, and the bending of DNA by Sac7d is associated with an increase in enthalpy of ∼14 kcal/mol.

REFERENCES

1. Travers, A. A. (1990) Why bend DNA? *Cell 60*, 177−180.
2. Harrington, R. E. (1992) DNA curving and bending in protein-DNA recognition, *Mol. Microbiol. 6*, 2549−2555.
3. Travers, A. A. (1995) in *DNA-Protein*: *Structural Interactions* (Lilley, D. M. J., Ed.) pp 49−75, IRL Press, New York.
4. Werner, M., Gronenborn, A. M., and Clore, G. M. (1996) Intercalation, DNA kinking, and the control of transcription, *Science 271*, 778−784.
5. Dickerson, R. E., and Chiu, T. K. (1997) Helix bending as a factor in protein/DNA recognition, *Biopolymers 44*, 361−403.
6. Swinger, K. K., and Rice, P. A. (2004) IHF and HU: Flexible architects of bent DNA, *Curr. Opin. Struct. Biol. 14*, 28−35.
7. Schultz, S. C., Shields, G. C., and Steitz, T. A. (1991) Crystal structure of a CAP-DNA complex: The DNA is bent by 90°, *Science 253*, 1001−1007.
8. Rice, P. A., Yang, S., Mizuuchi, K., and Nash, H. A. (1996) Crystal structure of an IHF-DNA complex: A protein-induced DNA U-turn, *Cell 87*, 1295−1306.
9. Dickerson, R. E. (1998) DNA bending: The prevalence of kinkiness and the virtues of normality, *Nucleic Acids Res. 26*, 1906−1926.
10. Dragan, A. I., Klass, J., Read, C., Churchill, M. E., Crane-Robinson, C., and Privalov, P. L. (2003) DNA binding of a non-sequence-specific HMG-D protein is entropy driven with a substantial non-electrostatic contribution, *J. Mol. Biol. 331*, 795−813.
11. Kim, Y., Geiger, J. H., Hahn, S., and Sigler, P. B. (1993) Crystal structure of a yeast TBP/TATA-box complex, *Nature 365*, 512−520.
12. Robinson, H., Gao, Y.-G., McCrary, B. S., Edmondson, S. P., Shriver, J. W. and Wang, A. H.-J. (1998) The hyperthermophile chromosomal protein Sac7d sharply kinks DNA, *Nature 392*, 202−205.
13. Zhang, Y., Xi, Z., Hegde, R. S., Shakked, Z., and Crothers, D. M. (2004) Predicting indirect readout effects in protein-DNA interactions, *Proc. Natl. Acad. Sci. U.S.A. 101*, 8337−8341.
14. Maher, L. J., III (1998) Mechanisms of DNA bending, *Curr. Opin. Chem. Biol. 2*, 688−694.
15. Parvin, J. D., McCormick, R. J., Sharp, P. A., and Fisher, D. E. (1995) Pre-bending of a promoter sequence enhances affinity for the TATA-binding factor, *Nature 373*, 724−727.
16. Travers, A. (2000) Recognition of distorted DNA structures by HMG domains, *Curr. Opin. Struct. Biol. 10*, 102−109.
17. Jen-Jacobson, L., Engler, L. E., and Jacobson, L. A. (2000) Structural and thermodynamic strategies for site-specific DNA binding proteins, *Struct. Folding Des. 8*, 1015−1023.
18. Peters, W. B., Edmondson, S. P., and Shriver, J. W. (2004) Thermodynamics of DNA binding and distortion by the hyperthermophile chromatin protein Sac7d, *J. Mol. Biol. 343*, 339−360.
19. Edmondson, S. P., Qiu, L., and Shriver, J. W. (1995) Solution Structure of the DNA-Binding Protein Sac7d from the Hyperthermophile *Sulfolobus acidocaldarius*, *Biochemistry 34*, 13289−13304.
20. Dragan, A. I., Read, C. M., Makeyeva, E. N., Milgotina, E. I., Churchill, M. E., Crane-Robinson, C., and Privalov, P. L. (2004) DNA binding and bending by HMG boxes: Energetic determinants of specificity, *J. Mol. Biol. 343*, 371−393.
21. Edmondson, S. P., and Shriver, J. W. (2001) DNA binding proteins Sac7d and Sso7d from *Sulfolobus*, *Methods Enzymol. 334*, 129−145.
22. Bedell, J. L., McCrary, B. S., Edmondson, S. P., and Shriver, J. W. (2000) The acid-induced folded state of Sac7d is the native state, *Protein Sci. 9*, 1878−1888.
23. McAfee, J., Edmondson, S., Datta, P., Shriver, J., and Gupta, R. (1995) Gene cloning, sequencing, expression, and characterization of the Sac7 DNA-binding proteins from the extremely thermophilic archaeon *Sulfolobus acidocaldarius*, *Biochemistry 34*, 10063−10077.
24. McAfee, J. G., Edmondson, S., Zegar, I., and Shriver, J. W. (1996) Equilibrium DNA binding of Sac7d protein from the hyperthermophile *Sulfolobus acidocaldarius*: Fluorescence and circular dichroism studies, *Biochemistry 35*, 4034−4045.
25. Bevington, P. R., and Robinson, D. K. (1992) *Data Reduction and Error Analysis for the Physical Sciences*, McGraw-Hill, New York.
26. McGhee, J., and von Hippel, P. (1974) Theoretical aspects of DNA-protein interactions: Co-operative and non-cooperative binding of large ligands to a one-dimensional homogeneous lattice, *J. Mol. Biol. 86*, 469−489.
27. Johnson, W. C., Jr. (1984) in *Food Analysis Principles and Techniques*, *Volume 2*, *Physicochemical Techniques* (Gruenwedel, D. W., and Whitaker, J. R., Eds.) Marcel Dekker, New York.
28. Savitsky, A., and Golay, M. J. E. (1964) Smoothing and differentiation of data by simplified least squares procedures, *Anal. Chem. 36*, 1627−1638.
29. Shriver, J., Peters, W., Szary, N., Clark, A., and Edmondson, S. (2001) Calorimetry of hyperthermophile proteins, *Methods Enzymol. 334*, 389−422.
30. Bundle, D. R., and Sigurskjold, B. W. (1994) Determination of accurate thermodynamics of binding by titration microcalorimetry, *Methods Enzymol. 247*, 288−305.
31. Kay, L. E., Keifer, P., and Saarinen, T. (1992) Pure absorption gradient enhanced heteronuclear single quantum correlation spectroscopy with improved sensitivity, *J. Am. Chem. Soc. 114*, 10663−10665.
32. Zhang, O., Kay, L. E., Olivier, J. P., and Forman-Kay, J. D. (1994) Backbone ^1H and ^{15}N resonance assignments of the N-terminal SH_3 domain of *drk* in folded and unfolded states using enhanced-sensitivity pulsed field gradient NMR techniques, *J. Biomol. NMR 4*, 845−858.

33. Markley, J. L., Bax, A., Arata, Y., Hilbers, C. W., Kaptein, R., Sykes, B. D., Wright, P. E., and Wuthrich, K. (1998) Recommendations for the presentation of NMR structures of proteins and nucleic acids, *J. Mol. Biol. 280*, 933−952.
34. Wishart, D. S., and Sykes, B. D. (1994) Chemical shifts as a tool for structure determination, *Methods Enzymol. 239*, 363−392.
35. Sreerama, N., and Woody, R. W. (2000) Estimation of protein secondary structure from CD spectra: Comparison of CONTIN, SELCON and CDSSTR methods with an expanded reference set, *Anal. Biochem. 282*, 252−260.
36. Gao, Y. G., Su, S. Y., Robinson, H., Padmanabhan, S., Lim, L., McCrary, B. S., Edmondson, S. P., Shriver, J. W., and Wang, A. H. (1998) The crystal structure of the hyperthermophile chromosomal protein Sso7d bound to DNA, *Nat. Struct. Biol. 5*, 782−786.
37. Su, S., Gao, Y. G., Robinson, H., Liaw, Y. C., Edmondson, S. P., Shriver, J. W., and Wang, A. H. (2000) Crystal structures of the chromosomal proteins Sso7d/Sac7d bound to DNA containing T-G mismatched base-pairs, *J. Mol. Biol. 303*, 395−403.
38. Makhatadze, G., and Privalov, P. L. (1995) Energetics of protein structure, *Adv. Protein Chem. 47*, 308−425.

BI047382W